Location and Radiological Features of the Synovial Pit and Its Usefulness in Hip Arthroscopy

Agustín O. Perea,* Ricardo Munafó Dauccia,* Ignacio Troncoso Pesoa**

*Hip Unit, Orthopedics and Traumatology Service, Sanatorio de La Trinidad, Autonomous City of Buenos Aires, Argentina **Orthopedics and Traumatology Service, CEMIC Hospital Universitario, Autonomous City of Buenos Aires, Argentina

ABSTRACT

Introduction: The synovial pit is a cystic lesion or notch in the femoral neck, initially regarded as an incidental finding but more recently associated with femoroacetabular impingement (FAI). It is observed in approximately 5% of the general population, with a higher prevalence in men, and in up to 33% of patients with FAI. Its identification is clinically relevant given its association with labral and articular cartilage damage, although its origin may be related to both femoral (cam) and acetabular (pincer) morphological abnormalities, making it difficult to attribute to a single cause. Materials and Methods: A total of 388 hip arthroscopies performed between 2018 and 2023 were included. Radiographs and complementary imaging studies were analyzed to classify morphological abnormalities and describe synovial pit characteristics. Measurements included the lateral center-edge angle, acetabular index, and alpha angle. Results: In patients with predominantly femoral abnormalities, impingement tended to occur more proximally, and the synovial pit was located in that region; conversely, when acetabular abnormalities predominated, impingement occurred more distally. No other variables reached statistical significance. Conclusion: The presence and features of the synovial pit in preoperative imaging, as well as its intraoperative identification during hip arthroscopy, may provide additional insight into the mechanisms of femoroacetabular impingement and its biomechanics.

Keywords: Synovial pit; femoroacetabular impingement; hip arthroscopy; imaging; pincer; cam.

Level of Evidence: IV

Ubicación y características radiológicas de la fosa sinovial y su utilidad en la artroscopia de cadera

RESUMEN

Introducción: La fosa sinovial es un quiste o una muesca en el cuello femoral, que inicialmente se consideró un hallazgo incidental, pero, en los últimos tiempos, se asocia con el impacto femoroacetabular. La prevalencia general de la fosa sinovial es del 5%, predomina en los hombres, y llega al 33% en pacientes con impacto femoroacetabular. Su identificación es relevante por la asociación con daño en el labrum y el cartílago articular, aunque su origen se relaciona tanto con trastornos morfológicos femorales (Cam) como acetabulares (Pincer), lo que dificulta atribuirlo a una causa específica. Materiales y Métodos: Se incluyeron 388 artroscopias de cadera realizadas entre 2018 y 2023, y se evaluaron radiografías y estudios complementarios para clasificar los trastornos morfológicos y las características de la fosa sinovial. Algunas de las mediciones fueron: ángulo de cobertura lateral, índice acetabular y ángulo alfa. Resultados: En los pacientes con predominio de trastorno femoral, la fricción sería más proximal; por ende, la fosa sinovial se encontraba en dicha zona; en cambio, cuando predomina el trastorno es acetabular, el conflicto sería más distal. El resto de las variables analizadas no alcanzaron un valor significativo. Conclusión: Las características de la fosa sinovial en los exámenes preoperatorios, como su identificación durante la artroscopia de cadera podrían ser un dato adicional para comprender el fenómeno de fricción y su biomecánica.

Palabras clave: Fosa sinovial; fricción femoroacetabular; artroscopia de cadera; diagnóstico por imágenes; Pincer; Cam. Nivel de Evidencia: IV

Received on November 26th, 2024. Accepted after evaluation on August 4th, 2025 • Dr. IGNACIO TRONCOSO PESOA • itroncosopesoa@gmail.com https://orcid.org/0000-0002-7879-0992

How to cite this article: Perea AO, Munafó Dauccia R., Troncoso Pesoa I. Location and Radiological Features of the Synovial Pit and Its Usefulness in Hip Arthroscopy. Rev Asoc Argent Ortop

Traumatol 2025;90(5):446-456. https://doi.org/10.15417/issn.1852-7434.2025.90.5.2069



INTRODUCTION

The synovial pit (SP), or synovial herniation pit, was first described by Michael J. Pitt in 1982. It is a small cystic or notched lesion in the femoral neck, of variable location and unknown origin, initially considered an incidental finding but, according to more recent studies, associated with a mechanical effect of femoroacetabular impingement (FAI).1-3

On imaging, SPs appear as rounded, oval, or occasionally multilobulated radiolucent lesions measuring < 10 mm, with a complete or incomplete thin sclerotic rim. They may contain homogeneous or heterogeneous soft-tissue material (synovial herniation) and are often accompanied by an inflammatory reaction.

The prevalence of SPs is approximately 5% in the general population and is higher in men.⁴ With the refinement of computed tomography (CT) and magnetic resonance imaging (MRI) for joint evaluation, the frequency of SP detection has increased significantly. Leunig et al. reported a prevalence of 33% in patients with FAI.5

Identifying an SP in the femoral neck can be useful given its association with FAI, as well as its correlation with labral and articular cartilage damage.

Since morphological abnormalities are usually mixed, it is difficult to attribute the appearance or development of SPs solely to femoral (Cam-type) or acetabular (Pincer-type) deformities. This raises several questions:

- Is there a relationship between SPs and the type of morphological abnormality?
- Is there a relationship between SPs and the degree of deformity or morphological abnormality?
- Is there a relationship between SPs and symptom severity or chronicity?
- Could understanding the characteristics of SPs aid in clinical management?

The objective of this study was to analyze the characteristics of SPs in patients with femoroacetabular impingement syndrome and to assess their usefulness in addressing the condition.

MATERIALS AND METHODS

Between 2018 and 2023, 388 hip arthroscopies were performed in our department. The primary diagnosis was femoroacetabular impingement syndrome. A retrospective observational study was conducted to analyze the presence and features of SPs.

The inclusion criterion was availability of CT or contrast-enhanced MRI (arthro-MRI) demonstrating the presence of an SP. The exclusion criteria were absence of surgical treatment, absence of an SP on imaging, or history of joint surgery (due to possible anatomic distortion).

A total of 23 patients (28 hips) met the inclusion criteria: 12 men (52.2%) and 11 women (47.8%). The mean age at surgery was 37.9 years (range, 22–52). The indication for hip arthroscopy was labral tear associated with FAI (Table 1).

All patients presented with hip pain and the diagnostic triad of clinical signs and imaging features consistent with FAI. A comprehensive clinical history and physical examination were performed. Radiographs of both hips (anteroposterior, lateral, and Dunn 45° views) were obtained, along with multi-slice CT with oblique axial cuts of the femoral head and neck, and arthro-MRI with a lidocaine test when indicated. The indication for arthroscopic surgery was based on an overall assessment of clinical and imaging findings.

During the procedure, the labrum was repaired and the morphological abnormality corrected. The SP was identified, and its location and morphology were documented (Figure 1). The following variables were evaluated:

Morphological abnormality: Radiographs were reviewed to classify deformities as Pincer, Cam, or Mixed. For acetabular overcoverage (Pincer), the lateral center-edge angle (Wiberg angle, normal 25°-40°) and the acetabular index (normal 0°-10°) were measured, as well as the acetabular wall crossover sign. For femoral deformity, the alpha angle was measured on the Dunn 45° projection, with <55° (Warwick) considered normal (Figure 2). All measurements were performed by imaging specialists not involved in the study.

SP analysis and location: Axial oblique CT or arthro-MRI slices were used. The center of rotation of the femoral head was determined by fitting a circle to the head contour, and the center of the SP was determined similarly. A line perpendicular to the femoral neck passing through the SP (line A) was drawn, and the distance from the femoral head center to line A (line B) was measured (Figure 3).

Table 1. Patient characteristics

Case	Age	Gen- der	Disor- der	Alpha (°)	CR- SP	SP Depth	SP Diam.	Rim	Shape	FH Diam.	Wiberg angle (°)	Tönnis angle	Osteoar- thritis
				()	(mm)	(mm)	(mm)			(mm)		8	(Tönnis)
1	46	F	Pincer	49	29	5	4	Complete	Rounded	44	31	3	0
2	52	F	Mixed	59	16	8	10	Complete	Oval	41	35	0	0
3	31	M	Mixed	63	13	3	3	Incomplete	Rounded	50	42	0	0
4	41	F	Mixed	62	8	5	5	Complete	Rounded	45	28	8	1
5	41	F	Mixed	65	6	6	6	Complete	Rounded	46	28	7	1
6	25	M	Mixed	58	10	5	4	Incomplete	Rounded	48	33	6	0
7	48	F	Mixed	55	9	9	10	Complete	Rounded	47	33	5	0
8	31	F	Mixed	76	9	6	7	Complete	Multilobulated	44	36	3	0
9	31	F	Mixed	73	15	3	5	Complete	Multilobulated	44	35	3	0
10	33	M	Cam	71	12	10	10	Complete	Rounded	53	30	5	1
11	24	M	Mixed	56	28	7	5	Complete	Rounded	46	40	0	0
12	33	F	Pincer	46	12	3	2	Complete	Rounded	40	24	10	1
13	33	M	Mixed	60	12	8	12	Complete	Oval	48	35	3	0
14	36	F	Mixed	60	13	14	8	Complete	Multilobulated	42	41	0	0
15	36	F	Mixed	61	12	11	6	Complete	Rounded	42	40	1	0
16	38	M	Mixed	72	8	9	7	Complete	Rounded	44	30	4	0
17	36	M	Mixed	58	14	5	5	Incomplete	Rounded	43	41	0	1
18	22	M	Mixed	53	19	6	8	Incomplete	Rounded	44	34	1	0
19	46	F	Pincer	45	13	4	6	Complete	Rounded	42	30	5	0
20	25	M	Mixed	55	17	6	11	Incomplete	Oval	44	38	0	1
21	46	F	Mixed	57	7	6	4	Complete	Rounded	43	43	0	0
22	25	M	Mixed	65	8	6	5	Complete	Rounded	46	28	8	0
23	37	M	Mixed	55	7	8	7	Complete	Rounded	48	28	3	0
24	50	M	Mixed	67	10	3	3	Complete	Rounded	47	29	5	0
25	50	M	Mixed	73	11	5	3	Complete	Rounded	47	27	5	0
26	51	F	Mixed	65	10	6	3	Complete	Rounded	44	30	6	0
27	51	F	Mixed	63	11	6	7	Complete	Rounded	44	30	6	0
28	42	F	Mixed	55	10	2	2	Complete	Rounded	48	42	0	1

F = female; M = male; CR-SP (mm) = distance from the center of rotation to the synovial pit; SP Depth (mm) = depth of the synovial pit; SP Diam. (mm) = diameter of the synovial pit; FH Diam (mm) = diameter of the femoral head.



Figure 1. Arthroscopic view of synovial pit.

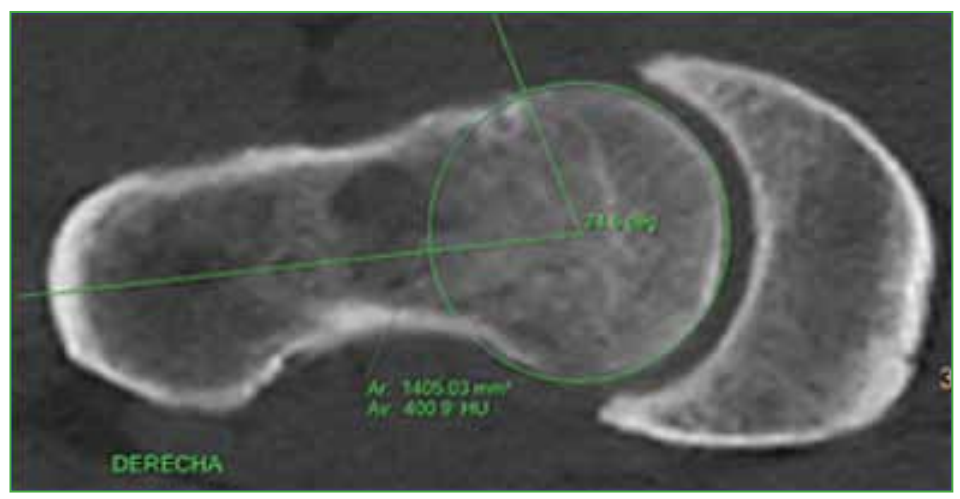


Figure 2. Alpha angle measurement.

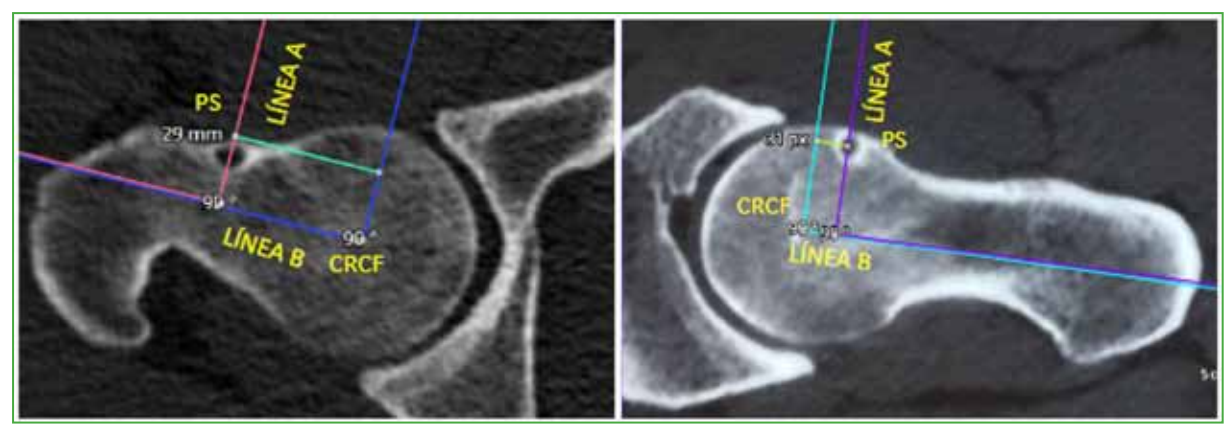


Figure 3. Analysis and location of the SP (distance from the center of rotation of the femoral head to the femoral pit).

SP morphology: The following parameters were analyzed on axial oblique CT or arthro-MRI slices: 1) measured by a tangent from the anterior femoral cortex to the deepest point of the SP (Figure 4); 2) measured by a tangent from the proximal femoral border to the most distal point of the SP (Figure 5); 3) Shape: round, oval, or multilobulated; and 4) Rim: complete (cyst) or incomplete (notched).

Symptom duration and sports activity: Measured from symptom onset to surgery; sports activity was recorded as frequency and type.



Figure 4. Depth of the synovial pit.

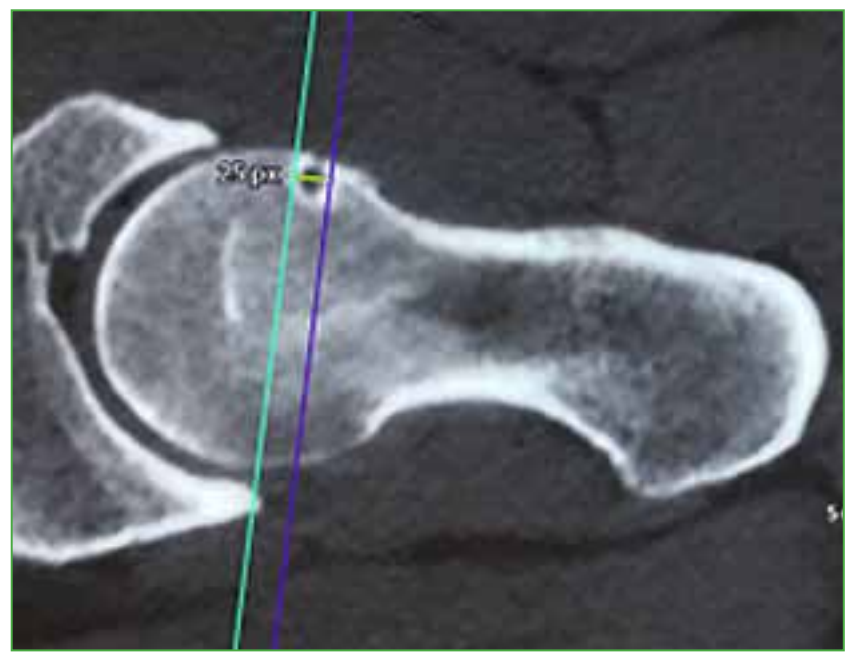


Figure 5. Femoral pit diameter.

RESULTS

In all statistical analyses, confidence intervals (CI) were calculated at 95%.

The type of morphological abnormality was analyzed: 85.71% had a mixed-type deformity (24 cases); 3.57% had a Cam-type deformity (1 case); and 10.71% had a Pincer-type deformity (3 cases). With regard to femoral disorder, the mean alpha angle was 60.6° (range, 45-76), mean Wiberg angle 33.6° (range, 24-46), and mean acetabular inclination (Tönnis angle) 3.5° (range, 0-10).

The mean distance from the SP to the femoral head center was 12.5 mm (range, 6–28); mean depth 6.3 mm (range, 2–14); and mean diameter 6 mm (range, 2–12). Eighty-two point one percent of SPs had complete rims, and 17.9% incomplete rims. The shape was round in 78.6% (22 cases), oval in 10.7% (3 cases), and multilobulated in 10.7% (3 cases).

The mean femoral head diameter was 45.1 mm. Seventy-five percent of patients had Tönnis grade 0 osteoarthritis and 25% grade 1; none had advanced OA (grades 2–3).

The mean duration from symptom onset to surgery was 13 months (range, 5–24). Seventy-two percent were active athletes (>3 sessions per week). The most frequent sport was soccer (44%), followed by functional training or gymnastics (35%); the remainder practiced other sports less frequently.

Statistical analyses are shown in Tables 2-4.

Table 2. Simple general statistical analysis

Simple statistics									
Variable n Mean Standard Median Minimum Maximun deviation									
Alpha angle	25	62.28000	6.64279	61.00000	53.00000	76.00000			
Distance between center of rotation and synovial pit	25	11.80000	4.69929	11.0000	6.00000	28.00000			

Table 3. Analysis of Spearman's overall correlation coefficient

Spearman correlation coefficients, $n = 25 \text{ Prob} > r $ assuming H0: Rho = 0							
Alpha angle Distance between center of rotation and synovial pit							
Alpha angle	1.00000	-0.21705 0.2973					
Distance between center of rotation and synovial pit	-0.21705 0.2973	1.00000					

Table 4. Analysis of Kendall's overall tau correlation coefficient.

Kendall's tau correlation coefficients b. n = 25 Prob > tau assuming H0: Tau = 0							
Alpha angle Distance between center of rotation and synovial pit							
Alpha angle	1.00000	-0.17864 0.2290					
Distance between center of rotation and synovial pit	-0.17864 0.2290	1.0000					

Correlation between alpha angle (Cam-type) and distance from the femoral head center was evaluated using Spearman and Kendall tests (Spearman = -0.21; 95% CI -0.54-0.19; Kendall = -0.17), showing a trend toward shorter distances with greater deformity, without statistical significance (Tables 5-7).

Table 5. Simple statistical analysis in patients with Cam-type disorder.

Variable	n	Mean	Standard deviation	Median	Minimum	Maximum
Wiberg angle	27	33.74074	5.52333	33.00000	24.00000	43.00000
Tönnis angle	27	3.40741	3.00332	3.00000	0	10.00000
Distance between center of rotation and synovial pit	27	12.48148	5.50787	11.00000	6.00000	29.00000

Table 6. Analysis of the overall Spearman correlation coefficient in patients with Cam-type disorder

Spearman correlation coefficients, n = 27 Prob > r assuming H0: Rho = 0								
	Wiberg's angle	Tönnis angle	Distance between center of rotation and synovial pit					
Wiberg angle	1.00000	-0.86986 <0.0001	0.37267 0.0556					
Tönnis angle	-0.86986 <0.0001	1.00000	-0.49373 0.0089					
Distance between center of rotation and synovial pit	0.37267 0.0556	-0.49373 0.0089	1.00000					

Table 7. Kendall's tau correlation coefficient analysis in patients with Cam-type disorder

Kendall's tau correlation coefficients b, n = 27 Prob > tau assuming HO: Tau = 0								
	Wiberg angle	Tönnis angle	Distance between center of rotation and synovial pit					
Wiberg angle	1.00000	-0.73900 <0.0001	0.25564 0.0734					
Tönnis angle	-0.73900 <0.0001	1.00000	-0.36264 0.0139					
Distance between center of rotation and synovial pit	0.25564 0.0734	-0.36264 0.0139	1.00000					

For Pincer-type deformities, Wiberg (Spearman = 0.37; 95% CI 0.00-0.66) and Tönnis angles (Spearman = -0.49; 95% CI -0.73 to -0.11) were correlated with distance from the femoral head center (Tables 8 and 9), suggesting that larger Wiberg angles correspond to greater distances and higher Tönnis angles to shorter distances (Table 3).

Table 8. Statistical analysis in patients with Pincer-type disorder.

Variable	n	Mean	Standard deviation	Sum	Minimum	Maximum
Alpha angle	28	60.80714	7.98303	1697	45.00000	76.00000
Depth	28	6.25000	2.68914	175.00000	2.00000	14.00000
Diameter	28	6.00000	2.76218	188.00000	2.00000	12.00000
Femoral head diameter	28	45.14286	2.87665	1264	40.00000	53.00000
Wiberg angle	28	33.60714	5.46598	941.00000	24.00000	43.00000
Tönnis angle	28	3.46420	2.96251	97.00000	0	10.00000

Table 9. Pearson's statistical analysis in patients with Pincer-type disorder.

	Pearson correlation coefficients, $n=28\ Prob> r $ assuming HO: Rho = 0							
	Alpha angle	Depth	Diameter	Femoral head diameter	Wiberg angle	Tönnis angle		
Alpha angle	1.00000	0.12551 0.5245	0.02855 0.8853	0.32348 0.0931	-0.08176 0.6792	0.10040 0.6112		
Depth	0.12551 0.5245	1,00000	0.62826 0.0003	-0.05267 0.7901	0.15055 0.4444	-0.21502 0.2719		
Diameter	0.02855 0.8853	0.62826 0.0003	1.00000	0.0652600.7415	0.07850 0.6913	-0.22178 0.2567		
Femoral head diameter	0.32348 0.0931	-0.05267 0.7901	0.06526 0.7415	1.00000	-0.05047 0.7987	0.05712 0.7728		
Wiberg angle	-0.08176 0.6792	0.15055 0.4444	0.07850 0.6913	-0.05047 0.7987	1.00000	-0.08785 <0.0001		
Tönnis angle	0.10040 0.6112	-0.21502 0.2719	-0.22178 0.2567	0.05712 0.7728	-0.08806 <0.0001	1.00000		

The correlations between the alpha angle, the Wiberg angle, and the Tönnis angle and the FS diameter and depth were analyzed, and a χ^2 test was applied to assess independence between rim type and FS imaging characteristics (Table 10). Specifically, there was no correlation between the alpha angle and diameter (p = 0.8853), between the Wiberg angle and diameter (p = 0.6913), or between the Tönnis angle and diameter (p = 0.2567). Likewise, no correlations were found between the alpha angle and depth (p = 0.5245), between the Wiberg angle and depth (p = 0.4444), or between the Tönnis angle and depth (p = 0.2719). By contrast, a significant association was observed between FS diameter and depth (Spearman = 0.63; 95% CI, 0.33-0.82; p = 0.0003), indicating that larger diameters were accompanied by greater depths, and vice versa (Table 11).

Table 10. Simple statistical analysis of the correlation between the alpha angle, Wiberg angle, and Tönnis angle with the diameter and depth of the synovial pit.

	Simple statistics								
Variable	n	Mean	Standard deviation	Sum	Minimum	Maximum			
Symptoms	28	12.67857	4.73015	355.00000	5.00000	24.00000			
Diameter	28	6.00000	2.76218	168.00000	2.00000	12.00000			
Femoral head diameter	28	45.14286	2.87665	1264	53.00000	53.00000			
Depth	28	6.25000	2.68914	175.00000	14.00000	14.00000			

Table 11. Analysis of Pearson correlation coefficients between the alpha angle, Wiberg angle, and Tönnis angle with the diameter and depth of the synovial pit.

Pearson correlation coefficients $n=28\ Prob> r $ assuming H0: Rho = 0								
	Symptoms	Diameter	Femoral head diameter	Depth				
Symptoms	1.00000	-0.03969 0.8411	0.00350 0.9859	0.08226 0.6773				
Diameter	-0.03969 0.8411	1.00000	0.06526 0.7415	0.62826 0.0003				
Femoral head diameter	0.00350 0.9859	0.06526 0.7415	1.00000	-0.05267 0.7901				
Depth	0.08226 0.6773	0.62826 0.0003	-0.05267 0.7901	1.00000				

The correlation between symptom duration (in months) and SP diameter was analyzed, as well as between symptom duration and depth, using the χ^2 test between the median number of months with symptoms and the rim type, and between the median number of months with symptoms and the morphological characteristics of the SP (Table 12). It was concluded that the null hypothesis could not be rejected, meaning that there is no correlation between the duration of symptoms and SP diameter (p = 0.8411), nor between the duration of symptoms and SP depth (p = 0.6773). The null hypothesis of independence between the median number of months of symptoms and the rim characteristics was also tested and not rejected (p = 0.2283); therefore, both variables were considered independent (Table 13). Likewise, the null hypothesis of independence between symptom duration and the imaging characteristics of the SP was not rejected (p = 0.2854), indicating that these variables were also independent.

Table 12. Analysis of the correlation between symptoms (months) and diameter and between symptoms (months) and depth.

Fisher's exact test	
Cell (1,1) Frequency (F)	15
Left aligned Pr ≤ F	0.9382
Right-aligned Pr ≥ F	0.2901
Probability table (P)	0.2283
Two-tailed Pr ≤ P	0.3531

Table 13. Hypothesis of independence between the median of the months of symptoms and the characteristics of the rims.

Fisher's exact test	
Cell (1,1) Frequency (F)	1
Left aligned Pr ≤ F	0.3358
Right-aligned $Pr \ge F$	0.9496
Probability table (P)	0.2854
Two-tailed $Pr \le P$	0.5433

DISCUSSION

In the early 1980s, Allen H. described a depression in the superolateral femoral neck ("Allen's cervical depression") associated with a local inflammatory reaction. Angel had previously referred to it as a "reaction area" in 1964.

The reaction area hypothesis proposed a mechanical origin due to capsular contact.⁸ The lesion was thought to result from mechanical and abrasive forces exerted by the thick joint capsule and the lateral band of the iliofemoral ligament, mainly during hip extension, causing synovial tissue herniation into cortical defects of the femoral neck.⁹

Years later, Leunig et al. retrospectively compared 117 hips from 101 consecutive patients with FAI against 132 hips from 105 consecutive patients with acquired dysplasia without impingement. They found SPs in 33% of the FAI group and in none of the dysplasia group, demonstrating a clear association.⁵

Therefore, SPs likely result from repetitive trauma and femoral neck impingement rather than being incidental findings, as initially believed. Leunig et al. also proposed that they represent juxta-articular fibrocystic changes rather than true synovial herniations. On radiographs, they appear as small (<10 mm) round or oval radiolucent lesions with sclerotic margins; on MRI, they show homogeneous or heterogeneous hyperintensity depending on content. Differential diagnoses include intraosseous ganglion, osteoid osteoma, and degenerative cyst. Few studies have analyzed the imaging features of SPs. Wang et al. evaluated 21 SPs in 18 patients, 17 of which were round (2 oval, 2 figure-eight shaped), and only 2 measured >10 mm.⁴

The question remains: what is the clinical usefulness of understanding their specific characteristics?

FAI syndrome is a complex, multifactorial, and dynamic condition, and any information that improves understanding of its pathogenesis and correction is valuable.

Recent technological advances have led to the development of preoperative and intraoperative tools such as *Stryker HipMap* (a patient-specific preoperative 3D analysis to support surgical planning) and *Stryker HipCheck* (an intraoperative guidance system to help localize and treat impingement precisely). It would be appealing to consider SP characteristics as potential guides for decision-making using conventional imaging, without the need for additional complex tools.

In our series, the incidence of SP was 7.2% among all hip arthroscopies (including dysplasia cases), explaining the lower rate compared to Leunig et al.⁵

According to our statistical analysis, when the Cam-type deformity predominates, impingement occurs more proximally; hence, the SP tends to appear in that region. Conversely, in Pincer-dominant cases, the conflict occurs more distally. Other variables (symptoms and imaging features) were not statistically significant. Larger-scale studies are required to confirm these findings.

Study limitations include the small sample size, the relatively low incidence of SPs in FAI patients, and potential selection bias. Participants may have been selected in a way that is not representative of the general population, limiting generalizability to broader populations or settings due to the specific characteristics of the sample or the setting in which the study was conducted.

CONCLUSION

The identification and characterization of SPs on preoperative imaging and during hip arthroscopy may provide additional insights into the mechanics of femoroacetabular impingement and the specific biomechanical environment of the hip joint.

Conflicts of interest: The authors declare no conflicts of interest.

A. O. Perea ORCID ID: https://orcid.org/0000-0002-7011-8966
R. Munafó Dauccia ORCID ID: https://orcid.org/0000-0003-0300-7841

REFERENCES

- Pitt M. Herniation pit of the femoral neck. AJR Am J Roentgenol 1982;138(6):1115-21. https://doi.org/10.2214/ajr.138.6.1115
- 2. Kavanagh L, Byrne C, Kavanagh E, Eustace S. Symptomatic synovial herniation pit-MRI appearances pre and post treatment. *BJR Case Rep* 2017;3(2):20160103. https://doi.org/10.1259/bjrcr.20160103
- Panzer S, Augat P, Esch U. CT assessment of herniation pits: prevalence, characteristics, and potential association with morphological predictors of femoroacetabular impingement. *Eur Radiol* 2008;18:1869-75. https://doi.org/10.1007/s00330-008-0952-7
- 4. Gao Z, Yin J, Ma L, Wang J, Meng Q. Clinical imaging characteristics of herniation pits of the femoral neck. *Orthop Surg* 2009;1(3):189-95. https://doi.org/10.1111/j.1757-7861.2009.00029.x
- Leunig M, Beck M, Kalhor M, Kim YJ, Werlen S, Ganz R. Fibrocystic changes at anterosuperior femoral neck: prevalence in hips with femoroacetabular impingement. *Radiology* 2005;236(1):237-46. https://doi.org/10.1148/radiol.2361040140
- 6. Kim JA, Park JS, Jin W, Ryu K. Herniation pits in the femoral neck: a radiographic indicator of femoroacetabular impingement? *Skeletal Radiol* 2011;40:167-72. https://doi.org/10.1007/s00256-010-0962-9
- 7. Ali Amjad, Ahmed Tarek Hafez, Adeel Nawab Ditta, Waqar Jan. Synovial pit of the femoral neck: a rare disease with rare presentations. *J Surg Case Rep* 2020;2020(6):rjaa195. https://doi.org/10.1093/jscr/rjaa195
- 8. Munafo Dauccia R. Tratamiento artroscópico de las lesiones del labrum acetabular. Estudio prospectivo de 68 casos con un seguimiento máximo de 9 años. *Artrosc (B. Aires)* 2011;18(1):8-18. Available at: https://pesquisa.bvsalud.org/portal/resource/pt/lil-610342
- Borody C. Symptomatic herniation pit of the femoral neck: a case report. J Manipulative Physiol Ther 2005;28(6): 449-51. https://doi.org/10.1016/j.jmpt.2005.06.003